Hydraulic differences between flowers and leaves are driven primarily by pressure-volume traits and water loss

Yi-Dong An[1], Adam B. Roddy [2], Tian-Hao Zhang[1]
and Guo-Feng Jiang [1]*

[1]Guangxi Key Laboratory of Forest Ecology and Conservation, Guangxi Colleges and Universities Key Laboratory for Cultivation and Utilization of Subtropical Forest Plantation, and State Key Laboratory for Conservation and Utilization of Subtropical Agro-Bioresources, College of Forestry, Guangxi University, Nanning, Guangxi, China, [2]Institute of Environment, Department of Biological Sciences, Florida International University, Miami, FL, United States

Flowers are critical for successful reproduction and have been a major axis of diversification among angiosperms. As the frequency and severity of droughts are increasing globally, maintaining water balance of flowers is crucial for food security and other ecosystem services that rely on flowering. Yet remarkably little is known about the hydraulic strategies of flowers. We characterized hydraulic strategies of leaves and flowers of ten species by combining anatomical observations using light and scanning electron microscopy with measurements of hydraulic physiology (minimum diffusive conductance (g_{min}) and pressure-volume (PV) curves parameters). We predicted that flowers would exhibit higher g_{min} and higher hydraulic capacitance than leaves, which would be associated with differences in intervessel pit traits because of their different hydraulic strategies. We found that, compared to leaves, flowers exhibited: 1) higher g_{min}, which was associated with higher hydraulic capacitance (C_T); 2) lower variation in intervessel pit traits and differences in pit membrane area and pit aperture shape; and 3) independent coordination between intervessel pit traits and other anatomical and physiological traits; 4) independent evolution of most traits in flowers and leaves, resulting in 5) large differences in the regions of multivariate trait space occupied by flowers and leaves. Furthermore, across organs intervessel pit trait variation was orthogonal to variation in other anatomical and physiological traits, suggesting that pit traits represent an independent axis of variation that have as yet been unquantified in flowers. These results suggest that flowers, employ a drought-avoidant strategy of maintaining high capacitance that compensates for their higher g_{min} to prevent excessive declines in water potentials. This drought-avoidant strategy may have relaxed selection on intervessel pit traits and allowed them to vary independently from other anatomical and physiological traits. Furthermore, the independent evolution of floral and foliar anatomical and physiological traits highlights their modular development despite being borne from the same apical meristem.

1 Introduction

Flowers play a crucial role during the reproductive phase of angiosperms, and their importance during this period has influenced angiosperm diversification and spread (Crane et al., 1995; Sprengel, 1996; Sargent and Ackerly, 2008). Producing and maintaining flowers requires the allocation of resources, such as water, carbon, and nutrients (Bazzaz et al., 1987; Reekie and Bazzaz, 1987a; Reekie and Bazzaz, 1987b; Reekie and Bazzaz, 1987c). Though these physiological costs of flowers are often assumed to be minimal in the context of the whole plant, resource limitation or stressful abiotic conditions can exacerbate the costs of producing and maintaining flowers (Lambrecht, 2013; Burkle and Runyon, 2016; Waser and Price, 2016; Bourbia et al., 2020; Harrison Day et al., 2022). The abiotic conditions that influence the physiological costs also act as agents of selection on floral traits and, in general, can be as strong an agent of selection on flowers as pollinators (Ashman and Schoen, 1994; Galen et al., 1999; Caruso, 2006; Lambrecht and Dawson, 2007; Teixido and Valladares, 2014; Lambrecht et al., 2017; Roddy et al., 2018; Caruso et al., 2019; Roddy et al., 2019; Kuppler and Kotowska, 2021a; Kuppler et al., 2021b). One of the most important resources for plant growth and reproduction is water, and the frequency and severity of droughts is increasing globally (Adams et al., 2017; Choat et al., 2018; Brodribb et al., 2020). These droughts potentially threaten food production and other ecosystem services that rely on flowering. Thus, maintaining water balance is critical to flower functioning, successful reproduction, and flower and fruit development (Galen et al., 1999; Lambrecht, 2013; Roddy et al., 2016; Zhang et al., 2018; Bourbia et al., 2020).

Like leaves, flowers are terminal structures often located in the hottest and driest parts of the plant crown, meaning they are exposed to similar evaporative environments as leaves (Blanke and Lovatt, 1993; Roddy and Dawson, 2012). In order to optimize photosynthesis in leaves, plants must prevent declines in water content, which requires coordination in the structural traits governing water flow through each component of the plant hydraulic pathway (Brodersen et al., 2014; Jupa et al., 2017; Li et al., 2019; Song et al., 2021; Fontes et al., 2022). For example, coordination between leaf vein density and stomatal density is nearly ubiquitous across studies and highlights the important roles that leaf veins and stomata play in coordinating liquid and vapor fluxes through the leaf to maintain water balance (Sack and Frole, 2006; Brodribb et al., 2007; Noblin et al., 2008; Boyce et al., 2009; Brodribb and Cochard, 2009; de Boer et al., 2012). However, over short timescales, water loss can exceed water supply, causing declines in water potentials in the xylem. Under extreme cases, excessive water loss and low water potentials can pull air into the xylem vessels from either outside the xylem or from adjacent, already embolized vessels, leading to the spread of air embolisms and xylem dysfunction (Dixon and Joly, 1895; Sperry and Tyree, 1988; Lens et al., 2011; Tyree and Zimmermann, 2013).

One of the major determinants of both the vulnerability of the xylem to embolism spread and also the efficiency of water flow through the xylem is the structure of intervessel pits and pit membranes that connect adjacent xylem conduits. Pit membranes, in particular, can be responsible for 50% or more of the total hydraulic resistance in the xylem (Wheeler et al., 2005; Choat et al., 2006; Hacke et al., 2006; Pittermann et al., 2006; Kaack et al., 2019). Comparative studies have shown that pit morphology can vary in terms of pit and pit aperture size, pit shape, and pit density, and that these pit traits can correlate with vessel diameter, vessel wall thickness, and photosynthetic rates, and vary both among species and among habitats (Schmitz et al., 2007; Lens et al., 2011; Jacobsen et al., 2016; Li et al., 2019; Zhang et al., 2021). In general, larger pit membranes are associated with higher hydraulic conductivity but are more vulnerable to embolism (Choat et al., 2005; Wheeler et al., 2005; Ellmore et al., 2006; Hacke et al., 2006; Lens et al., 2011). Furthermore, pit aperture shape can also influence embolism resistance: species with more cavitation-resistant branches exhibit narrower and more elliptical pit apertures (Lens et al., 2011; Scholz et al., 2013; Li et al., 2019). Thus, intervessel pit traits are important factors influencing both hydraulic safety and efficiency (Hacke et al., 2009; Jansen et al., 2009; Blackman et al., 2010; Li et al., 2016; Zhang et al., 2021), though they have not been systematically quantified in reproductive organs.

Compared to leaves, relatively little is known about the hydraulic traits of flowers, despite their importance to reproduction for most species (Gleason, 2018). Flowers have, at most, very few stomata (Lipayeva, 1989; Roddy et al., 2016; Zhang et al., 2018), meaning that water loss occurs primarily *via* diffusion across the cuticle (Roddy, 2019), and very low vein densities compared to leaves (Roddy et al., 2013; Zhang et al., 2018). As a result, minimum diffusive conductance (g_{min}) (Kerstiens, 1996) is strongly coordinated with petal vein density and hydraulic conductance, suggesting that g_{min} is critical to floral water balance and hydraulic conductance (Roddy et al., 2016). This has important implications for water balance during drought conditions. While leaves can close their stomata to limit water loss (Meinzer, 2002), without stomata flowers are likely unable to curtail water loss (Roddy et al., 2016; Roddy, 2019), which can cause them to lose more water during drought than leaves (Lambrecht, 2013; Bourbia et al., 2020). Thus, flower water potentials may decline more quickly than leaf water potentials and possibly cause air embolisms to spread more quickly through the xylem in flowers than in leaves (Zhang and Brodribb, 2017; Bourbia et al., 2020), depending on the morphology of intervessel pit traits in flowers and leaves (Zhang et al., 2021). However, hydraulic capacitance can buffer declines in water potentials that lead to embolism spread, and flowers have significantly higher hydraulic capacitance than leaves (Roddy et al., 2019). Since flowers are short-lived but have high water demands (Roddy and Dawson, 2012; Lambrecht, 2013; Roddy et al., 2018; Bourbia et al., 2020), flowers might employ different hydraulic strategies than leaves and stems and exhibit different coordination between hydraulic traits than leaves. High water demands and greater reliance on stored water may physiologically buffer flowers from diurnal variability in the water status of other plant structures. Prior evidence based on 132 species has suggested that vegetative and reproductive structures may be developmentally modular, with independent evolution of vein density in flowers and leaves (Roddy et al., 2013). Similarly, based on data from about 20 species, flowers

tend to have higher water contents and hydraulic capacitance than leaves. These differences in venation and pressure-volume traits may be linked to other differences in hydraulic anatomy and physiology. Yet remarkably little is known about the hydraulic strategies of flowers and their mechanisms of maintaining water balance.

In the present study, we characterized a diverse set of anatomical and physiological traits in both leaves and flowers of ten angiosperm species (Tables 1, 2). These traits included vein and stomatal traits, minimum diffusive conductance (g_{min}), parameters derived from pressure-volume curves (Scholander et al., 1965; Tyree and Hammel, 1972), and pit traits measured using scanning electron microscopy (SEM). We used this diverse set of traits to address the following questions (1) Do species with higher g_{min} have higher hydraulic capacitance, which could buffer water potential declines due to excessively high g_{min}? (2) Do flowers and leaves exhibit differences in intervessel pit structure reflecting their different hydraulic strategies? (3) Are anatomical and physiological traits in leaves and flowers coordinated, which would indicate similar hydraulic strategies? We hypothesized that flowers would exhibit higher g_{min} and higher hydraulic capacitance than leaves. Since flowers may rely on high water content and hydraulic capacitance to support high g_{min}, we also hypothesized that intervessel pit traits and the coordination of anatomical and physiological traits would differ in flowers and leaves and indicate different hydraulic strategies.

2 Materials and methods

2.1 Plant species and study site

Flower and leaf samples of the 10 species in this study (Figure 1 and Table 1) were collected on the campus of Guangxi University, Nanning (Guangxi, China, 22°50′N 108°17′E), which has a subtropical monsoon climate with a mean annual temperature of 21.8°C and a mean annual precipitation of 1,290 mm. Three to five randomly selected individuals per species were selected for

sampling. On each plant, a sun-exposed branch with leaves and flowers was cut and immediately placed in a bucket with water in the evening or early morning and transported back to the laboratory on campus.

2.2 Light microscopy of anatomical traits

All measurements were made on a fully expanded, healthy, sun-exposed branch with flowers and leaves for each of the 3-5 individuals sampled per species. From each leaf or flower, approximately 1-cm^2 sections of lamina were excised, avoiding the margin and midrib. These sections were cleared in a 1:1 solution of H_2O_2 (30%) and CH_3COOH (100%), then incubated at 70°C until all pigments had been removed. Sections were then removed from this solution and rinsed in water for 3 minutes, then the epidermises separated with forceps from the mesophyll and veins, allowing the upper and lower epidermises to be stained and mounted separately. To increase contrast, all samples were stained with Safranin O (0.5% w/v in water) for 5 min and Alcian Blue (1% w/v in 3% acetic acid) for 20 secs - 1 min, then washed in water and mounted on microscope slides.

Cross-sections of petals and leaves were made with a sliding microtome (RM225, Leica Inc., Germany) with a tissue thickness of 35 μm. Cross-sections with the same thickness were also made of peduncles and petioles. Sections were bleached for 10 min, rinsed in water, and then stained with Safranin O (0.5% w/v in water) for 5 min and with Alcian Blue (1% w/v in 3% acetic acid) for 20 secs - 1 min, rinsed, and then mounted on glass slides.

Images were taken at 5x, 10x, or 20x magnification, which had fields of view of approximately 3.99 mm^2, 0.89 mm^2, and 0.22 mm^2, respectively, using a compound microscope outfitted with a digital camera (DM3000, Leica Inc., Germany). Both abaxial (lower) and adaxial (upper) leaf and petal surfaces were imaged for all species to determine whether they were amphistomatous. In subsequent analyses, we used sum of abaxial and adaxial stomatal densities for comparisons. We found no stomata on petals of *Catharanthus roseus* and *Rosa* sp.

TABLE 1 List of species in this study.

Species	Family	Genus	Code
Bauhinia × blakeana Dunn	Fabaceae	*Bauhinia*	*Bb*
Bidens pilosa L.	Asteraceae	*Bidens*	*Bp*
Bougainvillea spectabilis Willd.	Nyctaginaceae	*Bougainvillea*	*Bs*
Catharanthus roseus (L.) G. Don	Apocynaceae	*Catharanthus*	*Cr*
Ceiba speciosa (A.St.-Hil.) Ravenna	Malvaceae	*Ceiba*	*Cs*
Hibiscus rosa-sinensis L.var. *rubro-plenus* Sweet	Malvaceae	*Hibiscus*	*Hr*
Michelia × alba DC.	Magnoliaceae	*Michelia*	*Ma*
Rhododendron sp.	Ericaceae	*Rhododendron*	*Rh*
Rosa sp.	Rosaceae	*Rosa*	*Ro*
Ruellia simplex C.Wright	Acanthaceae	*Ruellia*	*Rs*

TABLE 2 List of major characters with definition and units.

Symbol	Definition	Units
Minimum diffusive conductance and theoretical hydraulic conductivity		
$g_{min,area}$	Minimum diffusive conductance (normalized by the projected area of each organ)	mmol m^{-2} s^{-1}
$g_{min,mass}$	Minimum diffusive conductance (normalized by the dry mass of each organ)	mmol g^{-1} s^{-1}
K_{th}	Theoretical hydraulic conductivity	kg m^{-1} MPa^{-1} s^{-1}
Pressure–volume parameters		
C_T	Absolute capacitance, normalized by dry mass	mol kgs^{-1} MPa^{-1}
SWC	Saturated water content	g g^{-1}
Ψ_{sft}	Osmotic potential at full turgor	MPa
Ψ_{tlp}	Water potential at turgor loss point	MPa
SEM anatomical traits		
D_{pml}	Diameter of the outer pit membrane along the longest axis	μm
D_{pms}	Diameter of the outer pit membrane along the shortest axis	μm
D_{pal}	Diameter of the outer pit aperture along the longest axis	μm
D_{pas}	Diameter of the outer pit aperture along the shortest axis	μm
A_{pit}	Intervessel pit membrane surface area	μm^2
A_{pa}	Intervessel pit aperture surface area	μm^2
R_{pa}	Pit aperture shape = ratio of the longest axis of outer pit aperture to the shortest axis	
R_{pit}	Pit membrane shape = ratio of longest axis of outer pit membrane to the shortest axis	
D_p	Pit density = number of intervessel pits per vessel wall area	no.μm^{-2}
LM anatomical traits		
S_s	Stomatal size	μm^2
D_s	Stomatal density	no.mm^{-2}
D_v	Vein density	mm mm^{-2}
LT	Leaf thickness	μm
FT	Flower thickness	μm
D_h	Hydraulically-weighted vessel diameter	μm
T_w	Double vessel wall thickness	μm
VF	Vessel frequency	no.mm^{-2}

All anatomical measurements from images were made using ImageJ (Rueden et al., 2017). From images of paradermal sections, vein density (D_v) was measured as the total length of leaf or petal vascular tissue per mm^2 of leaf area or petal area, stomatal density (D_s) was measured by counting the number of stomata in the image and dividing by the area of the field of view, stomatal size (S_s) (comprising a pair of guard cells) was directly measured on at least five stomata per image. Partial stomata and epidermal cells were included in the density counts if visible along the top and left borders of the photomicrographs and discarded if visible along the bottom and right borders (Carins Murphy et al., 2017). Leaf and petal thicknesses were directly measured from the cross-section images.

Vessel double wall thickness (T_w) was measured on at least 10 pairs of connected vessels per image from cross-sections of peduncles and petioles. Mean hydraulically weighted vessel diameter (D_h) for each species was calculated as (Tyree and Zimmermann, 2013):

$$D_h = \left[\frac{\sum D^4}{N} \right]^{0.25}$$

where D is the equivalent circular diameter of a vessel whose area was calculated from its long and short diameters and N is the number of vessels measured. The D_h is biased towards wider vessels that conduct the majority of water according to the Hagen–Poiseuille law. Average vessel frequency (VF) was calculated per
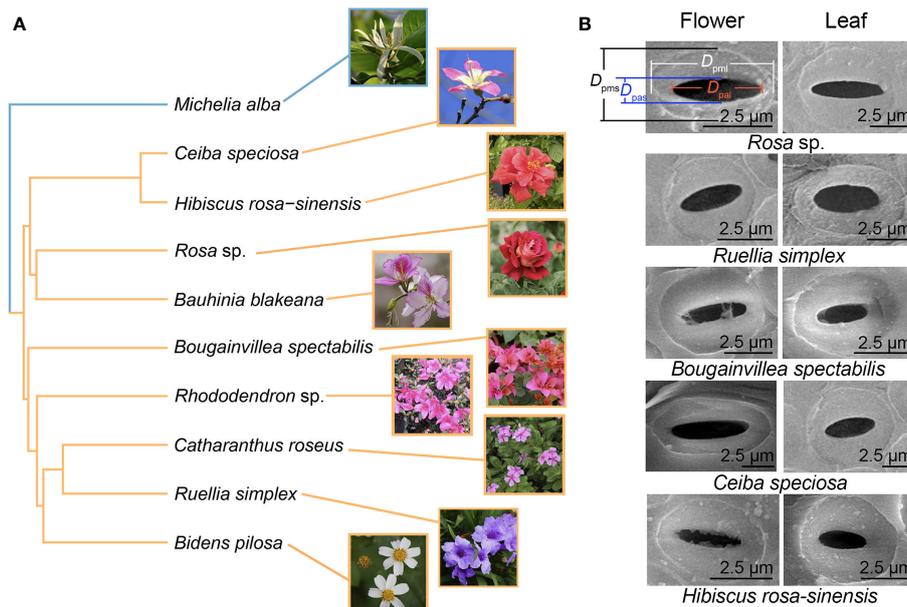
FIGURE 1
Phylogenetic relationships of the 10 species **(A)** and scanning electron micrographs of intervessel pits **(B)**. The bule and yellow branches represent magnoliids and eudicots, respectively.

image by dividing the total number of vessels by the image area. For each species, we calculated the theoretical hydraulic conductivity of as (Rakthai et al., 2020):

$$K_{th} = \frac{\pi \rho}{128 \eta} \times VF \times D_h^{4}$$

where ρ is fluid density (assumed to be 998.2 kg m^{-3} at 20°C) and η is viscosity of water (1.002 x 10^{-9} MPa s^{-1} at 20°C).

2.3 Scanning electron microscopy of anatomical traits

Upon returning samples to the lab, peduncles and petioles were immediately cut into small segments and placed in 100 ml of 5% FAA fixative (90:5:5 ratio of 70% ethanol, acetic acid, formaldehyde) at room temperature (25°C) to prevent expansion or shrinkage. Longitudinal sections of the segments were made with a sliding microtome (RM225, Leica Inc., Germany) at a thickness of 2-3 mm. The sections were fixed to aluminum sample holders with an electron-conductive carbon adhesive tape (Nisshin EM Co. Ltd., Tokyo), air-dried for 12 h at room temperature, and coated with gold using a sputter coater (Cressington 108Auto) for 40 secs at 0.08 mA to get a 20-nm-thick gold layer, under an argon atmosphere. A conventional scanning electron microscope (FEI Quattro S, US) with a voltage of 2 kV was used to visualize intervessel pit parameters according to standard protocols (Jansen et al., 2009; Lens et al., 2011; Zhang et al., 2021).

ImageJ (Rueden et al., 2017) was used to determine the following intervessel pit characteristics (Table 2): intervessel pit aperture surface area (A_{pa}), intervessel pit surface area or intervessel pit membrane surface area (A_{pit}), pit aperture longest diameter (D_{pal}), pit aperture shortest diameter (D_{pas}), pit aperture shape ($R_{pa} = D_{pal}/D_{pas}$), pit membrane longest diameter (D_{pml}), pit membrane shortest diameter (D_{pms}), pit shape or pit membrane shape ($R_{pit} = D_{pml}/D_{pms}$) and pit density ($D_{p}$). Mean values of these intervessel pit traits were calculated from at least 50 measurements from SEM images of various intervessel walls per individual.

2.4 Measurement of pressure–volume parameters

Shoots with leaves and flowers were collected from at least three individuals per species at night or at predawn and transported back to the laboratory. In the lab, all shoots were recut underwater to rehydrate for at least 2 h and covered with a black plastic bag during equilibration. Initial water potentials were checked and always close to -0.1 MPa. Pressure–volume curves were constructed for each sample by repeatedly measuring the bulk water potential using a pressure chamber (0.01 MPa resolution; PMS Instruments, Albany, OR, USA) and the mass to determine the relationship between water potential and water content following standard methods (Scholander et al., 1965; Tyree and Hammel, 1972; Sack and Pasquet-Kok, 2011; Roddy et al., 2019; Jiang et al., 2022). Prior to each water potential measurement, samples were enclosed in humidified plastic bags for about 20 min to allow equilibration. The pressure chamber was kept humidified with wet paper towels to prevent evaporation during the water potential measurement. After water potential measurement, the sample was weighed on a balance (± 0.0001g, model ML204T; Mettler Toledo). At the end of measurements, samples were oven-dried at 70°C for at least 72 h before determining dry mass. Because measuring flower surface area is difficult after turgor loss, pressure–volume parameters were

expressed on a dry mass basis, according to previous analyses (Roddy et al., 2019). From these pressure-violume curves, we calculated saturated water content (SWC), absolute capacitance (C_T), water potential at turgor loss point (Ψ_{tlp}), and osmotic potential at full turgor (Ψ_{sft}) (Table 2).

2.5 Leaf and flower minimum diffusive conductance

Shoots with leaves and flowers were collected at night from at least five individuals per species, recut underwater, and rehydrated over night while covered with a black plastic bag. Leaf and flower samples were excised in the morning, including the petiole or peduncle. Immediately following excision, their cut ends were sealed with glue and the entire organ was weighed every 10 min using an electronic balance (± 0.0001g, model ML204T; Mettler Toledo) in a dark room. The room was equipped with an air-conditioning to control the temperature and humidity, and samples were hung in front of a large fan as they desiccated. The velocity of air flow was high enough to physically move the samples. A small temperature and humidity sensor was kept near the samples, and temperature (T) and relative humidity (RH) were recorded manually each time a sample was weighed. After ten measurements, samples were scanned to determine projected area and then oven-dried at 70°C for 72 hours before determining dry mass.

Minimum diffusive conductance (g_{min}) was calculated as (Bourbia et al., 2020):

$$g_{min} = \frac{WL \cdot P_{atm}}{VPD}$$

where WL is the water loss rate (mmol m^{-2} s^{-1}) calculated as the slope of mass (g) over time (s) and normalized by the projected area (m^2) or dry mass (g) of each organ; P_{atm} is the atmospheric pressure (101.3 kPa); VPD is the vapor pressure deficit determined using the Arden Buck equation (Buck, 1981).

$$VPD = (1 - \frac{RH}{100})(0.61121 \times e^{\frac{17.502T}{240.97+T}})$$

2.6 Data analysis

All statistical analyses were conducted in R (v. 4.0.3) (Core Team, 2022). Paired t-tests were used to determine differences between flowers and leaves. Differences of pit area and density among different plant lineages were tested through one-way ANOVA. We used linear regression and standard major axis (SMA) regression (R package 'smatr') to determine the relationships between traits (Warton et al., 2012). Principal component analysis (PCA) was carried out on centered and scaled trait data using the 'vegan' package. A phylogenetic tree was built using the R package 'V.PhyloMaker' and phylogenetic independent contrasts (PICs) were calculated using the 'pic' function in the R package 'ape' and PIC correlations tested using

linear regression. All statistical tests were considered significant at $P < 0.05$. In order to contextualize our measurements of inter-conduit pit traits on leaves and flowers, we compiled published data reporting pit membrane surface area (A_{pit}) and pit density (D_p) for a diverse set of vascular plants (Supplementary Table 1). We used this broad dataset to examine how pit membrane area and pit density vary among lineages and organs.

3 Results

3.1 Trait variation and physiological trait coordination

Minimum diffusive conductance (g_{min}) was significantly higher in flowers than in leaves, whether it was normalized by dry mass ($t = 5.48, P<0.001$) or by projected area ($t = 4.88, P<0.001$) (Figures 2A, B and Supplementary Table 2). In addition, traits from pressure-volume curves were also significantly higher in flowers than in leaves ($P< 0.01$) (Figures 2C–F and Supplementary Table 2).

SEM images were used to examine intervessel pits in peduncles and petioles (Figure 1B). Compared to petioles, peduncles had significantly smaller pit membrane diameters D_{pms} ($t = -2.36, P< 0.05$) and D_{pml} ($t = -2.86, P< 0.01$) and smaller pit area A_{pit} ($t = -3.09, P< 0.05$), as well as differences in pit aperture shape R_{pa} ($t = -2.16, P< 0.05$) (Figures 2G–J and Supplementary Table 2). However, pit aperture diameters D_{pas} ($t = -0.43, P > 0.05$) and D_{pal} ($t = -1.49, P > 0.05$) and pit aperture area A_{pa} ($t = -1.15, P > 0.05$) were not significantly different between petioles and peduncles (Supplementary Table 2). Pit membrane shape R_{pit} ($t = 0.41, P > 0.05$) and pit density D_p ($t = 2.02, P > 0.05$) were similar in peduncles and petioles (Supplementary Table 2). Peduncles and petioles differed significantly in the size of the pit membranes despite having similar pit aperture sizes (Figure 2 and Supplementary Table 2).

In leaves, $g_{min,mass}$ was positively correlated with Ψ_{tlp} ($R^2 = 0.56, P = 0.013$) and Ψ_{sft} ($R^2 = 0.50, P = 0.022$), which remained significant after accounting for shared evolutionary history (Figures 3A, B and Table 3). No similar relationships between $g_{min,area}$ or $g_{min,mass}$ and C_T in leaves (Figures 3C, D) or $g_{min,mass}$ and Ψ_{tlp} or Ψ_{sft} in flowers (Figures 3E, F) were found. $g_{min,area}$ was positively correlated with C_T in flowers ($R^2 = 0.50, P = 0.034$, Figure 3H). The relationships between C_T and both $g_{min,mass}$ and $g_{min,area}$ were significant after accounting for shared evolutionary history (Table 3).

3.2 Trade off among intervessel pit traits

Pit density D_p was negatively correlated with pit membrane diameters D_{pms} ($R^2 = 0.68, P< 0.001$) and D_{pml} ($R^2 = 0.71, P< 0.001$) and with pit area A_{pit} ($R^2 = 0.61, P< 0.001$), as well as with pit aperture diameters D_{pas} ($R^2 = 0.58, P< 0.001$) and D_{pal} ($R^2 = 0.5, P< 0.001$) and pit aperture area A_{pa} ($R^2 = 0.47, P< 0.001$) (Figure 4). These correlations remained significant after accounting for shared evolutionary history (all $P< 0.05$, Table 3). Comparing these data to previously published data from stems and leaves of a broad
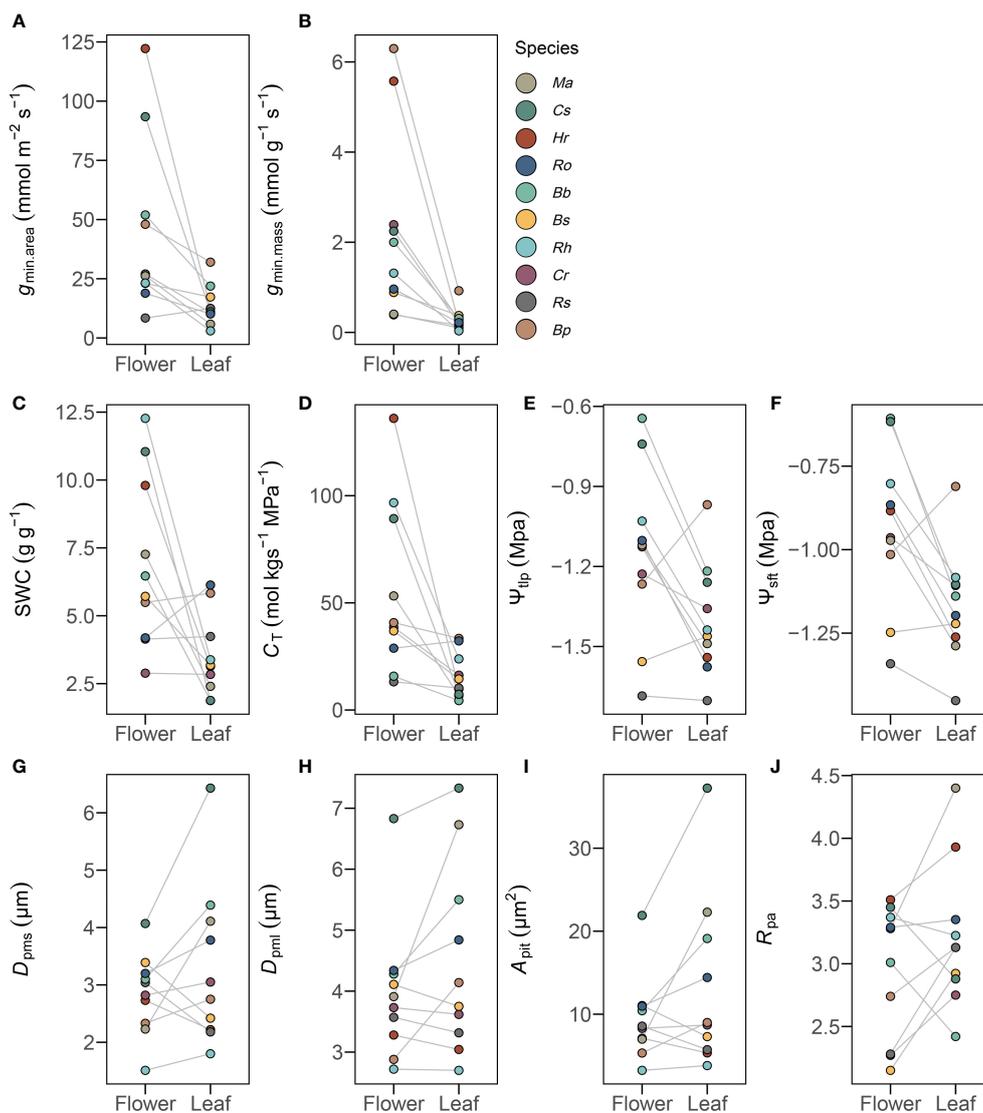
FIGURE 2
Traits differences of 10 selected traits for g_{min} **(A, B)**, pressure–volume curves **(C–F)**, and pit characteristics **(G–J)** in flowers and leaves. Mean values of listed traits from 10 species (n=10) were significantly different ($P< 0.05$) in flowers and leaves. See Table 2 for definitions of abbreviations.

sampling of angiosperms, gymnosperms, and ferns (Supplementary Table 1) showed that the negative correlation between D_p and A_{pit} was common (Supplementary Figure 1), with gymnosperms exhibiting larger pits that occur at lower density (Table 4 and Supplementary Figure 1). A_{pit} and D_p in flowers and leaves measured here were within the range reported previously for angiosperms and differed significantly from only gymnosperms (Table 4).

3.3 Relationships among pit traits and hydraulic traits

In petioles, like in other species (Lens et al., 2011; Mrad et al., 2018), K_{th} was positively correlated with D_{pas} ($R^2 = 0.45$, $P = 0.004$), D_{pal} ($R^2 = 0.58$, $P = 0.011$), and A_{pit} ($R^2 = 0.74$, $P = 0.001$), but in peduncles these relationships were not significant, mainly because

of the relatively constant D_{pas} and D_{pal} (Figures 5A-C). These correlations were statistically similar after accounting for shared evolutionary history ($P< 0.05$, Table 3). D_{pal} was positively correlated with D_h ($R^2 = 0.39$, $P = 0.003$) and with T_w ($R^2 = 0.45$, $P = 0.001$) in both petioles and peduncles (Figures 5D, E). These correlations remained significant only in leaves after accounting for shared evolutionary history ($P< 0.05$, Table 3). The positive relationships between D_{pal} and D_s ($R^2 = 0.25$, $P = 0.005$) (Figure 5G), A_{pit} and T_w ($R^2 = 0.49$, $P = 0.025$) (Figure 5F) became non-significant in leaves after accounting for shared evolutionary history (Table 3).

In peduncles, R_{pa} was positively correlated with D_h ($R^2 = 0.43$, $P = 0.04$), K_{th} ($R^2 = 0.43$, $P = 0.038$), SWC ($R^2 = 0.53$, $P = 0.018$), Ψ_{sft} ($R^2 = 0.54$, $P = 0.016$), Ψ_{tlp} ($R^2 = 0.50$, $P = 0.022$), C_T ($R^2 = 0.43$, $P = 0.041$), FT ($R^2 = 0.54$, $P = 0.015$) (Figures 6A-G). However, none of these correlations remained significant after accounting for shared evolutionary history (Table 3). R_{pa} was unrelated to any of these
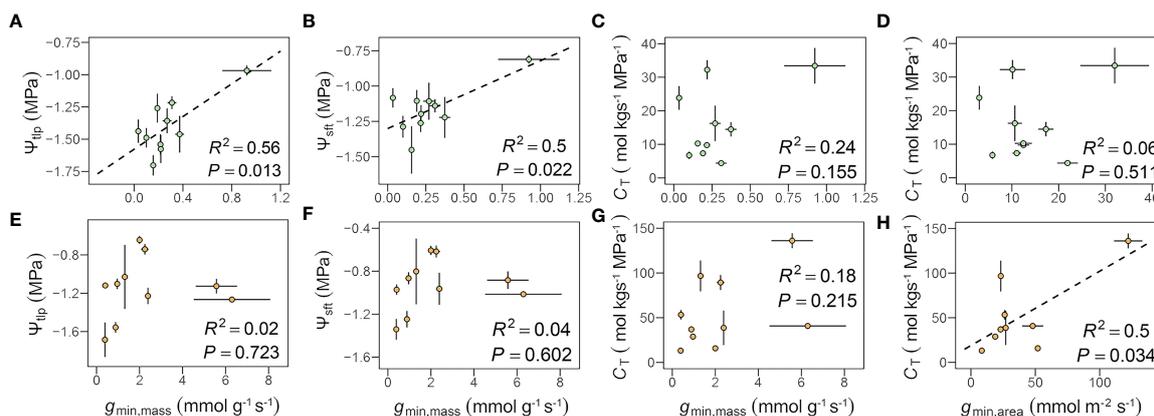
FIGURE 3
Relationships among minimum diffusive conductance (gmin) and traits from pressure-volume curves **(A–H**, see Table 2 for definitions of abbreviations.). Each point represents the mean value in peduncles and petiole, respectively. The green circles represent leaf, the orange circles represent flower, and error bars represent standard error (n = 5 individual plants).

hydraulic traits in petioles, but R_{pa} was positively correlated with leaf thickness after accounting for shared evolutionary history ($R^2 = 0.72$, $P < 0.01$) (Table 3). Only R_{pit} was negatively correlated with D_v ($R^2 = 0.42$, $P = 0.041$) (Figure 6H), even after accounting for shared evolutionary history ($R^2 = 0.72$, $P < 0.01$) (Table 3).

3.4 Phylogenetic independent contrast correlations of all paired traits between flowers and leaves

Phylogenetic independent contrast correlations (PIC) were made between all 24 traits measured in both flowers and leaves. Positive correlations of D_{pms} ($R^2 = 0.62$, $P = 0.012$), D_{pml} ($R^2 = 0.84$, $P = 0.001$), A_{pit} ($R^2 = 0.86$, $P < 0.001$), D_{pas} ($R^2 = 0.91$, $P < 0.001$), D_{pal} ($R^2 = 0.79$, $P = 0.001$), A_{pa} ($R^2 = 0.93$, $P < 0.001$), D_p ($R^2 = 0.78$, $P = 0.002$) between flowers and leaves were found (Figures 7A–G), and species with larger pit membranes and pit apertures in petioles also had larger pit membranes and pit apertures in peduncles (Supplementary Figure 2). Interestingly, pit membrane ($R^2 = 0.09$, $P = 0.444$) and pit aperture shape ($R^2 = 0.14$, $P = 0.33$) showed non-significant relationships after accounting for shared evolutionary history (Figures 7H, I).

There were positive correlations in traits between organs for S_s ($R^2 = 0.50$, $P = 0.048$), D_v ($R^2 = 0.41$, $P = 0.047$), T_w ($R^2 = 0.49$, $P = 0.024$), and $g_{min,mass}$ ($R^2 = 0.46$, $P = 0.031$) (Supplementary Figure 3), which became non-significant after accounting for shared evolutionary history (Table 5). Meanwhile some traits were not correlated among organs and remained uncorrelated even after accounting for shared evolutionary history: $g_{min,area}$ ($R^2 = 0.13$, $P = 0.336$), SWC ($R^2 = 0.07$, $P = 477$), K_{th} ($R^2 = 0.06$, $P = 0.523$), Ψ_{sft} ($R^2 = 0.44$, $P = 0.051$), C_T ($R^2 = 0.02$, $P = 0.721$), D_s ($R^2 = 0.13$, $P = 0.336$), and LT/FT ($R^2 = 0.04$, $P = 0.626$) (Table 5). Among physiological traits, only Ψ_{tlp} exhibited correlated evolution among flowers and leaves ($R^2 = 0.54$, $P = 0.024$) (Table 5).

3.5 Principal component analysis

The principal components analysis using all 24 traits revealed that the first two principal components explained 37.20% and 24.06% of the total variation, respectively. The first PC was driven by D_h, K_{th}, and some pit characters, including D_p, D_{pms}, and A_{pit}. The second PC was largely driven by pressure-volume parameters, including SWC, C_T, Ψ_{tlp}, Ψ_{sft}, as well as anatomical traits, including D_v, D_s, and LT. Flowers and leaves largely differed in the regions of trait space they occupied (Figure 8A).

Using only the pit traits in a principal components analysis revealed that the first two principal components explained 86.55% of the total variation among species and organs. The first PC (66.85%) was driven primarily by D_p versus all of the other pit traits except R_{pit} and R_{pa}. The second PC (19.70%) was driven primarily by R_{pit} and R_{pa}. There was a high level of overlap among flowers and leaves in the regions of pit trait space they occupied (Figure 8B).

4 Discussion

Our results revealed that despite large differences in g_{min} and pressure-volume traits between leaves and flowers, there were relatively small differences in pit traits between leaf petioles and flower peduncles (Figure 8). While flowers have higher g_{min} that is associated with higher hydraulic capacitance and higher turgor loss points than leaves (Figures 2, 3 and Supplementary Table 2), these differences in tissue water relations seem to be independent of differences in intervessel pit traits between organs. Thus, flowers rely on a cheap hydrostatic skeleton maintained by turgor pressure rather than a rigid, carbon-based skeleton (Roddy et al., 2019). High hydraulic capacitance of flowers prevents water potential declines that lead to xylem embolism and may have shielded selection from driving large divergences in intervessel pit traits between leaves and flowers.

		R^2	
		Flower	Leaf
D_p	D_{pml}	**0.93****	**0.90****
	D_{pms}	**0.89****	**0.89****
	A_{pit}	**0.95****	**0.86****
	D_{pal}	**0.84****	**0.84****
	D_{pas}	**0.93****	**0.85****
	A_{pa}	**0.84****	**0.81****
A_{pit}	A_{pa}	**0.92****	**0.92****
	D_h	0.26	**0.56***
K_{th}	D_{pas}	0.30	**0.71****
	D_{pal}	0.19	**0.79****
	A_{pit}	0.19	**0.87****
T_w	A_{pit}	0.001	0.43
D_{pal}	T_w	0.03	**0.49***
	D_h	0.34	**0.63***
	D_s	0.002	0.39
R_{pa}	D_h	0.17	0.04
	K_{th}	0.26	0.25
	SWC	0.37	0.22
	Ψ_{sft}	0.23	0.22
	Ψ_{tlp}	0.20	0.38
	C_T	0.26	**0.02**
	FT/LT	0.31	**0.72****
R_{pit}	D_v	0.02	**0.66****
$g_{min,mass}$	Ψ_{sft}	0.001	**0.50***
	Ψ_{tlp}	0.01	**0.45***
	C_T	**0.61***	0.72
$g_{min,area}$	C_T	**0.54***	0.17
VF	A_{pit}	0.10	0.09
	A_{pa}	0.19	0.09

The numbers represent the correlation coefficients, *: significant correlation (P < 0.05), **: significant correlation (P < 0.01), ***: significant correlation (P < 0.001).

4.1 Traits regulating water balance in flowers

In order for terminal organs to avoid desiccation, water loss must equal water supply, at least over diel timescales. In leaves, which maintain relatively high transpiration rates, the need to maintain water balance has resulted in coordinated evolution of

key anatomical traits that influence both liquid water supply and water vapor loss, particularly leaf vein density (D_v) and stomatal density and size (Sack et al., 2003; Brodribb et al., 2013; Simonin and Roddy, 2018; Zhang et al., 2018). While similar coordination between veins and stomata has been observed in flowers (Zhang et al., 2018), flowers often have few or no stomata, meaning that other traits, such as g_{min}, may be more important to regulating water balance (Roddy et al., 2016; Roddy, 2019). Furthermore, in both flowers and leaves, higher water contents and hydraulic capacitance can buffer water potential declines and lengthen the time required to reach steady state transpiration when water supply equals water loss (Simonin et al., 2013; Roddy et al., 2018; Roddy et al., 2019). Because flowers can have higher g_{min} than leaves (Figure 2), we predicted that there may be coordination between g_{min} and hydraulic capacitance, which would indicate that higher hydraulic capacitance can compensate for higher g_{min} in flowers. Across organs, g_{min} and hydraulic capacitance were correlated even after accounting for shared evolutionary history (Figure 3 and Table 3), with flowers having both higher g_{min} and higher capacitance than leaves (Figure 2). These patterns suggest that multiple traits and hydraulic strategies may be employed to maintain water balance among leaves and flowers.

In the absence of high hydraulic capacitance to buffer water potential declines, high g_{min} may cause water potentials to decline enough to initiate xylem embolism in flowers before leaves (Bourbia et al., 2020). If this were the case, we would predict that to prevent embolism in flowers, intervessel pit traits may have experienced selection to reduce embolism vulnerability. However, there were overall relatively small differences in intervessel pit traits between petioles and peduncles (Figure 2). One possible explanation is that intervessel pit traits may be shielded from selection by high hydraulic capacitance in flowers that allows g_{min} to be high without causing water potential declines and embolism spread. Because intervessel pit traits also influence hydraulic conductance (Choat et al., 2005; Ellmore et al., 2006; Hacke et al., 2006; Lens et al., 2011; Jacobsen et al., 2016), differences in intervessel pit traits between leaves and flowers may be due to divergent selection on hydraulic conductance among leaves and flowers. However, while flowers generally have relatively low hydraulic conductance, they are not necessarily outside the range of hydraulic conductance of leaves (Roddy et al., 2016), further suggesting that the strength of selection due to hydraulic efficiency acting on pit traits may be relatively weak.

4.2 Similar coordination of intervessel pit traits in leaves and flowers

In some cases, leaves and flowers exhibited similar coordination between intervessel pit traits despite the large morphological, anatomical, and physiological differences between these organs. We found similar coordination between A_{pit} and A_{pa} in both leaves and flowers (Figure 4), with larger A_{pit} being associated with higher theoretical hydraulic conductivity K_{th} in leaves (Figure 5). It is worth nothing that K_{th} incorporates only vessel traits and not
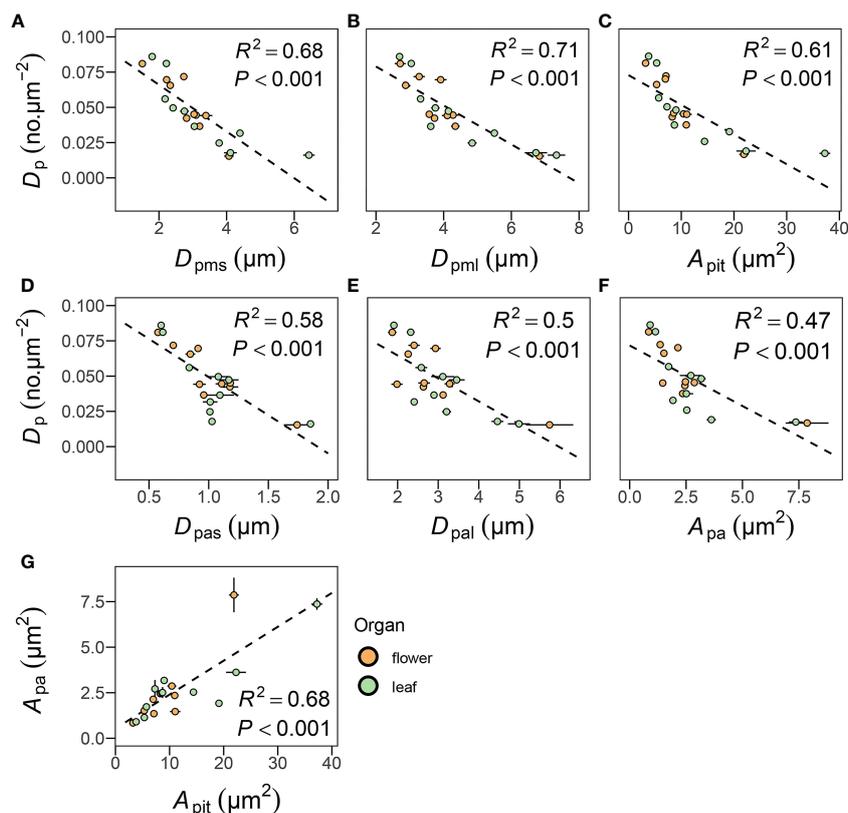
FIGURE 4

Relationships between pit density (D_p) and pit membrane **(A–C)** and pit aperture traits **(D–F)**, and relationships between pit membrane area (A_{pa}) with pit aperture area (A_{pit}) **(G)**. Each point represents the mean value in peduncles and petiole, respectively. The green circles represent leaf, the orange circles represent flower, and error bars represent standard error (n = 3-5 individual plants).

intervessel pit traits, so coordination between K_{th} and A_{pit} and A_{pa} suggests that variation in vessel size and density are linked to intervessel pit variation. A broad sampling of vascular plants (Supplementary Figure 1) revealed strong coordination between A_{pit} and pit density (D_p), due largely to packing constraints similar to those elucidated for stomata on the leaf surface and mesophyll cells inside the leaf (Franks and Beerling, 2009; Théroux-Rancourt et al., 2021; Borsuk et al., 2022; Jiang et al., 2023). Compared to other vascular plants, angiosperm A_{pit} and D_p were closer to the theoretical packing limit, which may be important to increasing hydraulic efficiency of angiosperm xylem regardless of other xylem traits.

Coordination between A_{pit} and D_p was also found among flower peduncles and leaf petioles, similar to other angiosperms, regardless of the fact that previously published data were taken from both stems and leaves (Supplementary Figure 1 and Supplementary Table 1). Previous studies have shown that larger A_{pit} is associated with larger A_{pa}, leading to higher hydraulic conductivity (Orians et al., 2004; Wheeler et al., 2005; Lens et al., 2011; Johnson et al., 2016). Similarly, we found that A_{pit} was positively linked to K_{th} in leaves but not in flowers (noted that A_{pit} was positively correlated with D_h but not VF in leaves, Table 3), suggesting that coordination in pit traits and vessel dimensions and packing were decoupled in flowers (Figure 5). Thus,

TABLE 4 Variation in D_p and A_{pit} among Fern, Gymnosperm and original data.

	A_{pit} (µm^2)	D_p (no.µm^{-2})
Fern	11.23 ± 3.65**a**	0.073 ± 0.0179**a**
Gymnosperm	174.74 ± 25.09**b**	0.004 ± 0.0008**b**
Leaf	13.29 ± 1.84**a**	0.045 ± 0.0043**a**
Flower	9.38 ± 0.90**a**	0.052 ± 0.0035**a**

Different lower-case letters following the values indicate significant differences between groups ($P < 0.05$, LSD's *post hoc* test, one-way ANOVA, values are means ± SE). Data for angiosperms, gymnosperms, and ferns were collected from published references (Table S1).
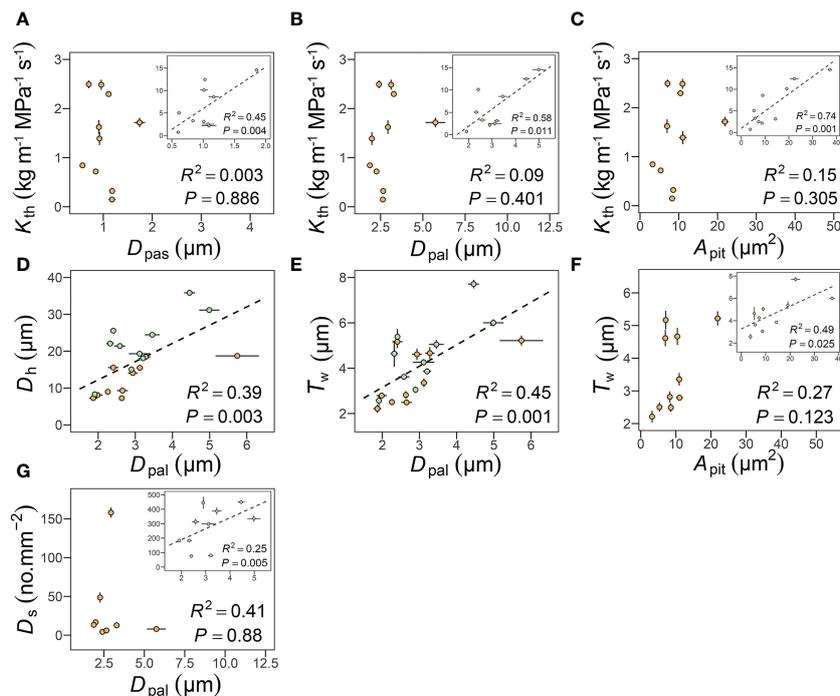
FIGURE 5
Relationships among pit apertures traits and theoretical hydraulic conductance (K_{th}) **(A, B)**, pit membrane area and K_{th} **(C)** and double vessel wall thickness (T_w) **(F)**, pit apertures traits and vessel diameter **(D)**, and double vessel wall thickness **(E)**, and stomatal density **(G)**. Each point represents the mean value in peduncles and petiole, respectively. The green circles represent leaf, the orange circles represent flower, and error bars represent standard error (n = 3-5 individual plants).
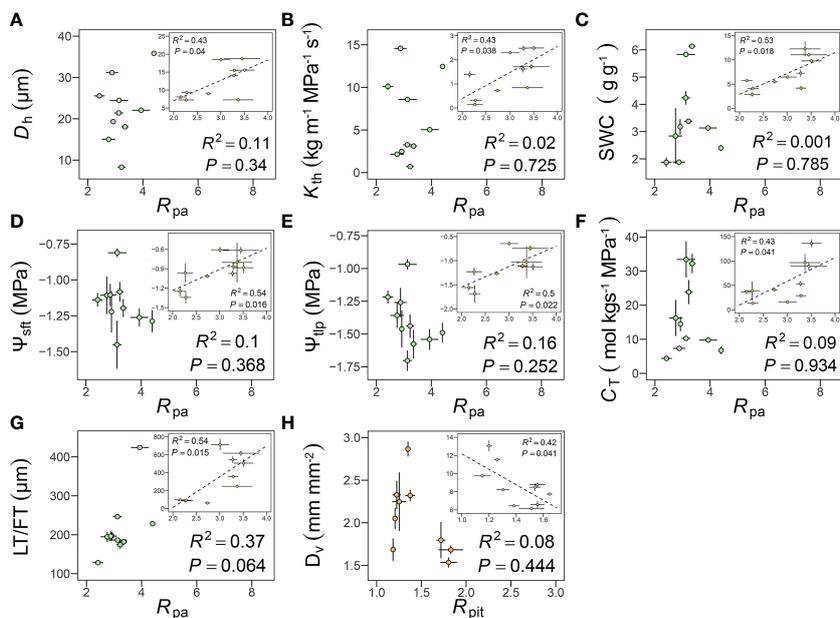
FIGURE 6
Relationships among pit membrane shape (R_{pit}), pit apertures shape (R_{pa}) and hydraulic traits. **(A–H**, see Table 2 for definitions of abbreviations). Each point represents the mean value in peduncles and petiole, respectively. The green circles represent leaf, the orange circles represent flower, and error bars represent standard error (n = 3-5 individual plants).
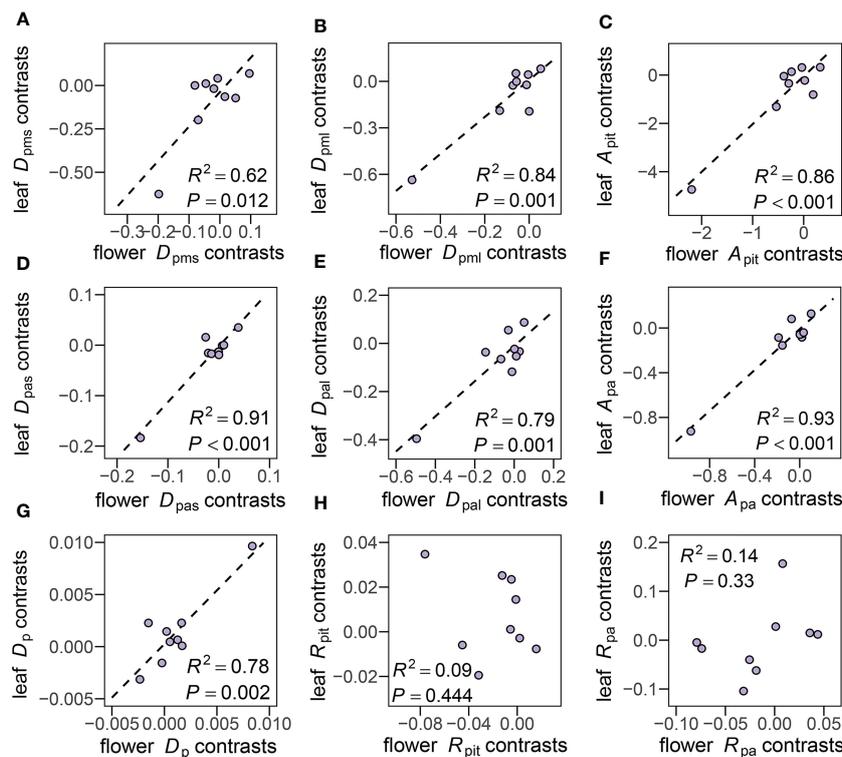
FIGURE 7
Phylogenetic independent contrast (PIC) correlations for pit traits. **(A–I**, see Table 2 for definitions of abbreviations) of the 10 species studied, showing the PICs calculated for pit traits between flowers and leaves. Correlation coefficients and P values are shown for statistically significant correlations based on Pearson's product-moment correlation.

despite obeying similar biophysical packing principles as vegetative organs–i.e. stomatal and vein densities (Zhang et al., 2018)–flowers can deviate in other traits that also influence hydraulic performance.

4.3 Special pit traits and correlations in flowers

From the hydraulic efficiency perspective, plants that have larger diameter vessels will have higher hydraulic efficiency (Hargrave et al., 1994; Christenhusz et al., 2011; Liu et al., 2019), while larger conduit diameter, larger pit membrane area, and larger pit aperture area, will be expected to decrease hydraulic safety (Pittermann et al., 2010; Lens et al., 2011; Brodersen et al., 2014; Jacobsen et al., 2016). Conduit wall thickness is thought increase hydraulic safety (Hacke et al., 2001; Brodribb and Holbrook, 2005). In our results, both pit membrane and pit aperture traits were correlated with K_{th} and D_h in leaves, no such correlations were found in flowers (Table 3). These results may indicate that leaves increase hydraulic efficiency with larger vessels and A_{pit}, but they may increase hydraulic safety through thicker vessel walls and more elliptical pits (Table 3). On the other hand, high hydraulic capacitance of flowers prevents water potential declines may relax the selective pressure of intervessel pit traits for hydraulic efficiency and safety. In general, elliptically shaped pit apertures are associated

with greater embolism resistance, with more cavitation-resistant species exhibiting narrower and more elliptical pit apertures (Lens et al., 2011; Scholz et al., 2013; Jacobsen et al., 2016). Consequently, angiosperms adapted to dry environments might have smaller conduit diameters and thicker, denser, smaller, and more elliptical pit apertures (Wheeler et al., 2005; Hacke et al., 2007; Jansen et al., 2009; Lens et al., 2011; Scholz et al., 2013). While intervessel pit traits might influence both hydraulic safety and efficiency, none of the pit traits were correlated with hydraulic traits in flowers (Table 3). It is highly likely, therefore, that traits exhibiting greater differences between leaves and flowers (e.g. pressure-volume traits) may be more important to flower water balance than intervessel pit traits.

Flowers have been shown to exhibit high diversity in hydraulic traits with higher water content and higher hydraulic capacitance than leaves (Roddy et al., 2019). We found similar patterns in our data, with flowers exhibiting greater variation in g_{min} and pressure-volume traits than leaves (Figure 2). However, flowers exhibited less variation in pit traits than leaves (Figure 2), although there were some clear differences in intervessel pit traits between leaves and flowers. This was further validated by the PCA results (Figure 8), in which R_{pit} and R_{pa} loaded on the same axis as the pressure-volume traits, in contrast to all other intervessel pit traits, which were orthogonal to other hydraulic traits except D_h and K_{th}. Further corroborating the role of R_{pit} and

TABLE 5 Phylogenetic independent contrast (PIC) correlations of all traits between flowers and leaves for the 10 species studied.

Trait	p-value	R^2
D_{pms}	<0.001	**0.62****
D_{pml}	0.001	**0.84****
A_{pit}	<0.001	**0.86****
D_{pas}	<0.001	**0.91****
D_{pal}	0.001	**0.79****
A_{pa}	<0.001	**0.93****
R_{pit}	0.444	0.09
R_{pa}	0.330	0.14
D_p	0.002	**0.78****
$g_{min,area}$	0.336	0.13
$g_{min,mass}$	0.203	0.22
SWC	0.477	0.07
K_{th}	0.523	0.06
Ψ_{sft}	0.051	0.44
Ψ_{tlp}	0.024	**0.54****
C_T	0.721	0.02
S_s	0.201	0.22
D_s	0.336	0.13
D_v	0.100	0.34
LT/FT	0.626	0.04
D_h	0.058	0.42
T_w	0.096	0.35
VF	0.101	0.34

The numbers represent the correlation coefficients, *, significant correlation (P < 0.05); **, significant correlation (P < 0.01); ***, significant correlation (P < 0.001).

R_{pa} in causing the divergence in hydraulic strategies between leaves and flowers, R_{pit} and R_{pa} exhibited no correlated evolution between leaves and flowers, in contrast to all other intervessel pit traits (Figure 7). Taken together, these results suggest that while most of the hydraulic differences between leaves and flowers is due to stomatal and vein anatomy and pressure-volume traits, differences in pit and pit aperture shape may also signify important differences.

5 Conclusions

The water dynamics of flowers are critical to successful reproduction and population viability, yet remarkably little is known about the hydraulic strategies of flowers and their mechanisms of maintaining water balance. Limiting water loss, storing large amounts of water, and building xylem safe from embolism are all ways of avoiding the detrimental effects of water limitation. Here we show that, compared to leaves, flowers are
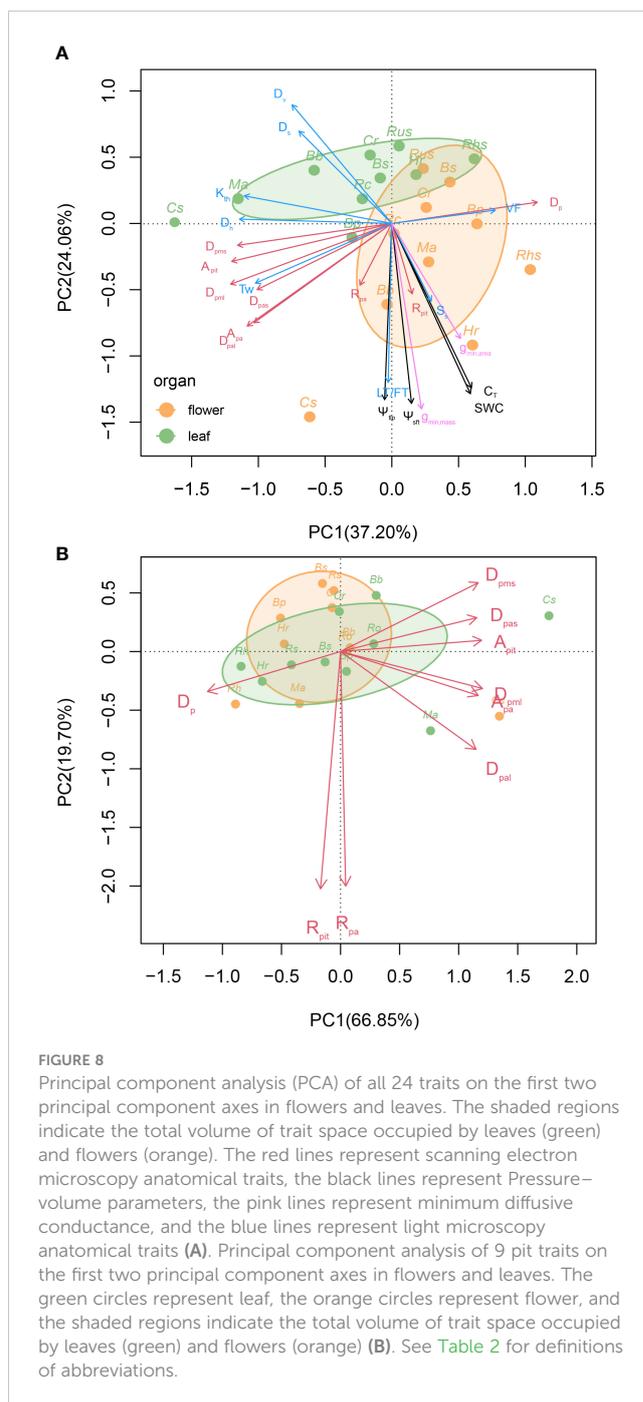

FIGURE 8
Principal component analysis (PCA) of all 24 traits on the first two principal component axes in flowers and leaves. The shaded regions indicate the total volume of trait space occupied by leaves (green) and flowers (orange). The red lines represent scanning electron microscopy anatomical traits, the black lines represent Pressure–volume parameters, the pink lines represent minimum diffusive conductance, and the blue lines represent light microscopy anatomical traits **(A)**. Principal component analysis of 9 pit traits on the first two principal component axes in flowers and leaves. The green circles represent leaf, the orange circles represent flower, and the shaded regions indicate the total volume of trait space occupied by leaves (green) and flowers (orange) **(B)**. See Table 2 for definitions of abbreviations.

leakier and exhibit relatively few differences in intervessel pit traits that influence embolism vulnerability. Instead, flowers primarily use high water contents to prevent water potential declines. This drought-avoidant strategy employed by flowers may have protected their xylem from selection for greater differences from leaves. Furthermore, by quantifying a broad suite of anatomical and physiological traits among leaves and flowers, we show that with the exception of pit and pit aperture shape, intervessel pit traits are largely orthogonal to stomatal and vein traits and pressure-volume traits. These results highlight the many dimensions in which flowers have diverged from leaves under different functional demands and suggest that high water content and hydraulic capacitance are the

primary traits that protect flowers from experiencing low water potentials that can cause failure in the hydraulic system.

Data availability statement

The original contributions presented in the study are included in the article/Supplementary Material. Further inquiries can be directed to the corresponding author.

Author contributions

G-FJ conceived the ideas and designed the study. Y-DA, AR and G-FJ collected the data. Y-DA, T-HZ and G-FJ analyzed the data. G-FJ and Y-DA wrote the first manuscript, AR helped to improve final manuscript; and all authors reviewed each draft before giving approval for submission of the final version. All authors contributed to the article and approved the submitted version.

Funding

Acknowledgments

Conflict of interest

The authors declare that the research was conducted in the absence of any commercial or financial relationships that could be construed as a potential conflict of interest.

Publisher's note

All claims expressed in this article are solely those of the authors and do not necessarily represent those of their affiliated organizations, or those of the publisher, the editors and the reviewers. Any product that may be evaluated in this article, or claim that may be made by its manufacturer, is not guaranteed or endorsed by the publisher.

Supplementary material

The Supplementary Material for this article can be found online at: https://www.frontiersin.org/articles/10.3389/fpls.2023.1130724/full#supplementary-material

References

Adams, H. D., Zeppel, M. J. B., Anderegg, W. R. L., Hartmann, H., Landhäusser, S. M., Tissue, D. T., et al. (2017). A multi-species synthesis of physiological mechanisms in drought-induced tree mortality. *Nat. Ecol. Evol.* 1 (9), 1285–1291. doi: 10.1038/s41559-017-0248-x

Ashman, T. L., and Schoen, D. J. (1994). How long should flowers live? *Nature* 371 (6500), 788–791. doi: 10.1038/371788a0

Bazzaz, F. A., Chiariello, N. R., Coley, P. D., and Pitelka, L. F. (1987). Allocating resources to reproduction and defense: new assessments of the costs and benefits of allocation patterns in plants are relating ecological roles to resource use. *BioScience* 37 (1), 58–67. doi: 10.2307/1310178

Blackman, C. J., Brodribb, T. J., and Jordan, G. J. (2010). Leaf hydraulic vulnerability is related to conduit dimensions and drought resistance across a diverse range of woody angiosperms. *New Phytol.* 188 (4), 1113–1123. doi: 10.1111/j.1469-8137.2010.03439.x

Blanke, M. M., and Lovatt, C. J. (1993). Anatomy and transpiration of the avocado inflorescence. *Ann. Bot.* 71 (6), 543–547. doi: 10.1006/anbo.1993.1070

Borsuk, A. M., Roddy, A. B., Theroux-Rancourt, G., and Brodersen, C. R. (2022). Structural organization of the spongy mesophyll. *New Phytol.* 234 (3), 946–960. doi: 10.1111/nph.17971

Bourbia, I., Carins-Murphy, M. R., Gracie, A., and Brodribb, T. J. (2020). Xylem cavitation isolates leaky flowers during water stress in pyrethrum. *New Phytol.* 227 (1), 146–155. doi: 10.1111/nph.16516

Boyce, C. K., Brodribb, T. J., Feild, T. S., and Zwieniecki, M. A. (2009). Angiosperm leaf vein evolution was physiologically and environmentally transformative. *Proc. R. Soc. B: Biol. Sci.* 276 (1663), 1771–1776. doi: 10.1098/rspb.2008.1919

Brodersen, C., Jansen, S., Choat, B., Rico, C., and Pittermann, J. (2014). Cavitation resistance in seedless vascular plants: the structure and function of interconduit pit membranes. *Plant Physiol.* 165 (2), 895–904. doi: 10.1104/pp.113.226522

Brodribb, T. J., and Cochard, H. (2009). Hydraulic failure defines the recovery and point of death in water-stressed conifers. *Plant Physiol.* 149 (1), 575–584. doi: 10.1104/pp.108.129783

Brodribb, T. J., Feild, T. S., and Jordan, G. J. (2007). Leaf maximum photosynthetic rate and venation are linked by hydraulics. *Plant Physiol.* 144 (4), 1890–1898. doi: 10.1104/pp.107.101352

Brodribb, T. J., and Holbrook, N. M. (2005). Water stress deforms tracheids peripheral to the leaf vein of a tropical conifer. *Plant Physiol.* 137 (3), 1139–1146. doi: 10.1104/pp.104.058156

Brodribb, T. J., Jordan, G. J., and Carpenter, R. J. (2013). Unified changes in cell size permit coordinated leaf evolution. *New Phytol.* 199 (2), 559–570. doi: 10.1111/nph.12300

Brodribb, T. J., Powers, J., Cochard, H., and Choat, B. (2020). Hanging by a thread? forests and drought. *Science* 368 (6488), 261–266. doi: 10.1126/science.aat7631

Buck, A. L. (1981). New equations for computing vapor pressure and enhancement factor. *J. Appl. Meteorology* 20 (12), 1527–1532. doi: 10.1175/1520-0450(1981)020<1527:Nefcvp>2.0.Co;2

Burkle, L. A., and Runyon, J. B. (2016). Drought and leaf herbivory influence floral volatiles and pollinator attraction. *Global Change Biol.* 22 (4), 1644–1654. doi: 10.1111/gcb.13149

Carins Murphy, M. R., Jordan, G. J., and Brodribb, T. J. (2017). Ferns are less dependent on passive dilution by cell expansion to coordinate leaf vein and stomatal spacing than angiosperms. *PloS One* 12 (9), e0185648. doi: 10.1371/journal.pone.0185648

Caruso, C. M. (2006). Plasticity of inflorescence traits in lobelia siphilitica (Lobeliaceae) in response to soil water availability. *Am. J. Bot.* 93 (4), 531–538. doi: 10.3732/ajb.93.4.531

Caruso, C. M., Eisen, K. E., Martin, R. A., and Sletvold, N. (2019). A meta-analysis of the agents of selection on floral traits. *Evolution* 73 (1), 4–14. doi: 10.1111/evo.13639

Choat, B., Brodie, T. W., Cobb, A. R., Zwieniecki, M. A., and Holbrook, N. M. (2006). Direct measurements of intervessel pit membrane hydraulic resistance in two angiosperm tree species. *Am. J. Bot.* 93 (7), 993–1000. doi: 10.3732/ajb.93.7.993

Choat, B., Brodribb, T. J., Brodersen, C. R., Duursma, R. A., López, R., and Medlyn, B. E. (2018). Triggers of tree mortality under drought. *Nature* 558 (7711), 531–539. doi: 10.1038/s41586-018-0240-x

Choat, B., Lahr, E. C., Melcher, P. J., Zwieniecki, M. A., and Holbrook, N. M. (2005). The spatial pattern of air seeding thresholds in mature sugar maple trees. *Plant Cell Environ.* 28 (9), 1082–1089. doi: 10.1111/j.1365-3040.2005.01336.x

Christenhusz, M. J. M., Reveal, J. L., Farjon, A., Gardner, M. F., Mill, R. R., and Chase, M. W. (2011). A new classification and linear sequence of extant gymnosperms. *Phytotaxa* 19, 55–70. doi: 10.11646/phytotaxa.19.1.3

Core Team, R. (2022). *R: a language and environment for statistical computing* (Vienna, Austria: R Foundation for Statistical Computing). Available at: https://www.R-project.org/.

Crane, P. R., Friis, E. M., and Pedersen, K. R. (1995). The origin and early diversification of angiosperms. *Nature* 374 (6517), 27–33. doi: 10.1038/374027a0

de Boer, H. J., Eppinga, M. B., Wassen, M. J., and Dekker, S. C. (2012). A critical transition in leaf evolution facilitated the Cretaceous angiosperm revolution. *Nat. Commun.* 3 (1), 1221. doi: 10.1038/ncomms2217

Dixon, H. H., and Joly, J. (1895). XII. on the ascent of sap. *Philos. Trans. R. Soc. London (B.)* 186, 563–576. doi: 10.1098/rstb.1895.0012

Ellmore, G. S., Zanne, A. E., and Orians, C. M. (2006). Comparative sectoriality in temperate hardwoods: hydraulics and xylem anatomy. *Botanical J. Linn. Soc.* 150 (1), 61–71. doi: 10.1111/j.1095-8339.2006.00510.x

Fontes, C. G., Pinto-Ledezma, J., Jacobsen, A. L., Pratt, R. B., and Cavender-Bares, J. (2022). Adaptive variation among oaks in wood anatomical properties is shaped by climate of origin and shows limited plasticity across environments. *Funct. Ecol.* 36 (2), 326–340. doi: 10.1111/1365-2435.13964

Franks, P. J., and Beerling, D. J. (2009). Maximum leaf conductance driven by CO2 effects on stomatal size and density over geologic time. *Proc. Natl. Acad. Sci.* 106 (25), 10343–10347. doi: 10.1073/pnas.0904209106

Galen, C., Sherry, R. A., and Carroll, A. B. (1999). Are flowers physiological sinks or faucets? costs and correlates of water use by flowers of polemonium viscosum. *Oecologia* 118 (4), 461–470. doi: 10.1007/s004420050749

Gleason, S. M. (2018). A blooming interest in the hydraulic traits of flowers. *Plant Cell Environ.* 41 (10), 2247–2249. doi: 10.1111/pce.13345

Hacke, U. G., Jacobsen, A. L., and Pratt, R. B. (2009). Xylem function of arid-land shrubs from California, USA: an ecological and evolutionary analysis. *Plant Cell Environ.* 32 (10), 1324–1333. doi: 10.1111/j.1365-3040.2009.02000.x

Hacke, U. G., Sperry, J. S., Feild, T. S., Sano, Y., Sikkema, E. H., and Pittermann, J. (2007). Water transport in vesselless angiosperms: conducting efficiency and cavitation safety. *Int. J. Plant Sci.* 168 (8), 1113–1126. doi: 10.1086/520724

Hacke, U. G., Sperry, J. S., Pockman, W. T., Davis, S. D., and McCulloh, K. A. (2001). Trends in wood density and structure are linked to prevention of xylem implosion by negative pressure. *Oecologia* 126 (4), 457–461. doi: 10.1007/s004420100628

Hacke, U. G., Sperry, J. S., Wheeler, J. K., and Castro, L. (2006). Scaling of angiosperm xylem structure with safety and efficiency. *New Phytol.* 26 (6), 689–701. doi: 10.1093/treephys/26.6.689

Hargrave, K. R., Kolb, K. J., Ewers, F. W., and Davis, S. D. (1994). Conduit diameter and drought-induced embolism in salvia mellifera Greene (Labiatae). *New Phytol.* 126 (4), 695–705. doi: 10.1111/j.1469-8137.1994.tb02964.x

Harrison Day, B. L., Carins-Murphy, M. R., and Brodribb, T. J. (2022). Reproductive water supply is prioritized during drought in tomato. *Plant Cell Environ.* 45 (1), 69–79. doi: 10.1111/pce.14206

Jacobsen, A. L., Tobin, M. F., Toschi, H. S., Percolla, M. I., and Pratt, R. B. (2016). Structural determinants of increased susceptibility to dehydration-induced cavitation in post-fire resprouting chaparral shrubs. *Plant Cell Environ.* 39 (11), 2473–2485. doi: 10.1111/pce.12802

Jansen, S., Choat, B., and Pletsers, A. (2009). Morphological variation of intervessel pit membranes and implications to xylem function in angiosperms. *Am. J. Bot.* 96 (2), 409–419. doi: 10.3732/ajb.0800248

Jiang, G. F., Li, S. Y., Dinnage, R., Cao, K. F., Simonin, K. A., and Roddy, A. B. (2023). Diverse mangroves deviate from other angiosperms in their genome size, leaf cell size, and cell packing density relationships. *Ann. Bot* 131, 347–360. doi: 10.1093/aob/mcac151

Jiang, G. F., Li, S. Y., Li, Y. C., and Roddy, A. B. (2022). Coordination of hydraulic thresholds across roots, stems, and leaves of two co-occurring mangrove species. *Plant Physiol* 189, 2759–2174. doi: 10.1093/plphys/kiac240

Johnson, D. M., Wortemann, R., McCulloh, K. A., Jordan-Meille, L., Ward, E., Warren, J. M., et al. (2016). A test of the hydraulic vulnerability segmentation hypothesis in angiosperm and conifer tree species. *Tree Physiol.* 36 (8), 983–993. doi: 10.1093/treephys/tpw031

Jupa, R., Plichta, R., Paschová, Z., Nadezhdina, N., and Gebauer, R. (2017). Mechanisms underlying the long-term survival of the monocot dracaena marginata under drought conditions. *Tree Physiol.* 37 (9), 1182–1197. doi: 10.1093/treephys/tpx072

Kaack, L., Altaner, C., Carmesin, C., Diaz, A., Holler, M., Kranz, C., et al. (2019). Function and three-dimensional structure of intervessel pit membranes in angiosperms: a review. *IAWA J.* 40, 673–702. doi: 10.1163/22941932-40190259

Kerstiens, G. (1996). Cuticular water permeability and its physiological significance. *J. Exp. Bot.* 47 (12), 1813–1832. doi: 10.1093/jxb/47.12.1813

Kuppler, J., and Kotowska, M. M. (2021a). A meta-analysis of responses in floral traits and flower–visitor interactions to water deficit. *Global Change Biol.* 27, 3095–3108. doi: 10.1111/gcb.15621

Kuppler, J., Wieland, J., Junker, R. R., and Ayasse, M. (2021b). Drought-induced reduction in flower size and abundance correlates with reduced flower visits by bumble bees. *AoB Plants* 13, 1–7. doi: 10.1093/aobpla/plab001

Lambrecht, S. C. (2013). Floral water costs and size variation in the highly SelfingLeptosiphon bicolor(Polemoniaceae). *Int. J. Plant Sci.* 174 (1), 74–84. doi: 10.1086/668230

Lambrecht, S. C., and Dawson, T. E. (2007). Correlated variation of floral and leaf traits along a moisture availability gradient. *Oecologia* 151 (4), 574–583. doi: 10.1007/s00442-006-0617-7

Lambrecht, S. C., Morrow, A., and Hussey, R. (2017). Variation in and adaptive plasticity of flower size and drought-coping traits. *Plant Ecol.* 218 (6), 647–660. doi: 10.1007/s11258-017-0718-x

Lens, F., Sperry, J. S., Christman, M. A., Choat, B., Rabaey, D., and Jansen, S. (2011). Testing hypotheses that link wood anatomy to cavitation resistance and hydraulic conductivity in the genus acer. *New Phytol.* 190 (3), 709–723. doi: 10.1111/j.1469-8137.2010.03518.x

Li, S., Hao, G. Y., Niinemets, U., Harley, P. C., Wanke, S., Lens, F., et al. (2019). The effects of intervessel pit characteristics on xylem hydraulic efficiency and photosynthesis in hemiepiphytic and non-hemiepiphytic ficus species. *Physiol. Plant* 167 (4), 661–675. doi: 10.1111/ppl.12923

Li, S., Lens, F., Espino, S., Karimi, Z., Klepsch, M., Schenk, H., et al. (2016). Intervessel pit membrane thickness as a key determinant of embolism resistance in angiosperm xylem. *IAWA J.* 37, 152–171. doi: 10.1163/22941932-20160128

Lipayeva, L. J. B. Z. (1989). On the anatomy of petals in angiosperms. *Botanicheskii Zhurnal* 74, 333, 9–18.

Liu, X., Liu, H., Gleason, S. M., Goldstein, G., Zhu, S., He, P., et al. (2019). Water transport from stem to stomata: the coordination of hydraulic and gas exchange traits across 33 subtropical woody species. *Tree Physiol.* 39 (10), 1665–1674. doi: 10.1093/treephys/tpz076

Meinzer, F. C. (2002). Co-Ordination of vapour and liquid phase water transport properties in plants. *Plant Cell Environ.* 25 (2), 265–274. doi: 10.1046/j.1365-3040.2002.00781.x

Mrad, A., Domec, J. C., Huang, C. W., Lens, F., and Katul, G. (2018). A network model links wood anatomy to xylem tissue hydraulic behaviour and vulnerability to cavitation. *Plant Cell Environ.* 41 (12), 2718–2730. doi: 10.1111/pce.13415

Noblin, X., Mahadevan, L., Coomaraswamy, I. A., Weitz, D. A., Holbrook, N. M., and Zwieniecki, M. A. (2008). Optimal vein density in artificial and real leaves. *Proc. Natl. Acad. Sci.* 105 (27), 9140–9144. doi: 10.1073/pnas.0709194105

Orians, C., Vuuren, M., Harris, N., Babst, B., and Ellmore, G. (2004). Differential sectoriality in long-distance transport in temperate tree species: evidence from dye flow, 15N transport, and vessel element pitting. *Trees* 18, 501–509. doi: 10.1007/s00468-004-0326-y

Pittermann, J., Choat, B., Jansen, S., Stuart, S. A., Lynn, L., and Dawson, T. E. (2010). The relationships between xylem safety and hydraulic efficiency in the cupressaceae: the evolution of pit membrane form and function. *Plant Physiol.* 153 (4), 1919–1931. doi: 10.1104/pp.110.158824

Pittermann, J., Sperry, J., Hacke, U., Wheeler, J., and Sikkema, E. (2006). Torus-Margo pits help conifers compete with angiosperms. *Sci. (New York N.Y.)* 310, 1924. doi: 10.1126/science.1120479

Rakthai, S., Fu, P. L., Fan, Z. X., Gaire, N. P., Pumijumnong, N., Eiadthong, W., et al. (2020). Increased drought sensitivity results in a declining tree growth of pinus latteri in northeastern Thailand. *Forests* 11 (3), 361. doi: 10.3390/f11030361

Reekie, E. G., and Bazzaz, F. A. (1987a). Reproductive effort in plants. 1. carbon allocation to reproduction. *Am. Nat.* 129 (6), 876–896. doi: 10.1086/284681

Reekie, E. G., and Bazzaz, F. A. (1987b). Reproductive effort in plants. 2. does carbon reflect the allocation of other resources? *Am. Nat.* 129 (6), 897–906. doi: 10.1086/284682

Reekie, E. G., and Bazzaz, F. A. (1987c). Reproductive effort in plants. 3. effect of reproduction on vegetative activity. *Am. Nat.* 129 (6), 907–919. doi: 10.1086/284683

Roddy, A. B. (2019). Energy balance implications of floral traits involved in pollinator attraction and water balance. *Int. J. Plant Sci.* 180 (9), 944–953. doi: 10.1086/705586

Roddy, A., Brodersen, C., and Dawson, T. (2016). Hydraulic conductance and the maintenance of water balance in flowers. *Plant Cell Environ.* 39, 2123–2132. doi: 10.1111/pce.12761

Roddy, A. B., and Dawson, T. E. (2012). Determining the water dynamics of flowering using miniature sap flow sensors. *Acta Hortic.* 951), 47–53. doi: 10.17660/ActaHortic.2012.951.4

Roddy, A. B., Guilliams, C. M., Lilittham, T., Farmer, J., Wormser, V., Pham, T., et al. (2013). Uncorrelated evolution of leaf and petal venation patterns across the angiosperm phylogeny. *J. Exp. Bot.* 64 (13), 4081–4088. doi: 10.1093/jxb/ert247

Roddy, A. B., Jiang, G. F., Cao, K., Simonin, K. A., and Brodersen, C. R. (2019). Hydraulic traits are more diverse in flowers than in leaves. *New Phytol.* 223 (1), 193–203. doi: 10.1111/nph.15749

Roddy, A. B., Simonin, K. A., McCulloh, K. A., Brodersen, C. R., and Dawson, T. E. (2018). Water relations of calycanthus flowers: hydraulic conductance, capacitance, and embolism resistance. *Plant Cell Environ.* 41 (10), 2250–2262. doi: 10.1111/pce.13205

Rueden, C. T., Schindelin, J., Hiner, M. C., DeZonia, B. E., Walter, A. E., Arena, E. T., et al. (2017). ImageJ2: ImageJ for the next generation of scientific image data. *BMC Bioinf.* 18 (1), 529. doi: 10.1186/s12859-017-1934-z

Sack, L., Cowan, P. D., Jaikumar, N., and Holbrook, N. M. (2003). The 'hydrology' of leaves: co-ordination of structure and function in temperate woody species. *Plant Cell Environ.* 26 (8), 1343–1356. doi: 10.1046/j.0016-8025.2003.01058.x

Sack, L., and Frole, K. (2006). LEAF STRUCTURAL DIVERSITY IS RELATED TO HYDRAULIC CAPACITY IN TROPICAL RAIN FOREST TREES. *Ecology* 87 (2), 483–491. doi: 10.1890/05-0710

Sack, L., and Pasquet-Kok, J. (2011) *Leaf pressure-volume curve parameters*. Available at: http://www.publish.csiro.au/prometheuswiki (Accessed 1 May 2014).

Sargent, R. D., and Ackerly, D. D. (2008). Plant-pollinator interactions and the assembly of plant communities. *Trends Ecol. Evol.* 23 (3), 123–130. doi: 10.1016/j.tree.2007.11.003

Schmitz, N., Jansen, S., Verheyden, A., Kairo, J. G., Beeckman, H., and Koedam, N. (2007). Comparative anatomy of intervessel pits in two mangrove species growing along a natural salinity gradient in gazi bay, Kenya. *Ann. Bot.* 100 (2), 271–281. doi: 10.1093/aob/mcm103

Scholander, P. F., Bradstreet, E. D., Hemmingsen, E. A., and Hammel, H. T. (1965). Sap pressure in vascular plants. *Science* 148 (3668), 339–346. doi: 10.1126/science.148.3668.339

Scholz, A., Rabaey, D., Stein, A., Cochard, H., Smets, E., and Jansen, S. (2013). The evolution and function of vessel and pit characters with respect to cavitation resistance across 10 prunus species. *Tree Physiol.* 33 (7), 684–694. doi: 10.1093/treephys/tpt050

Simonin, K. A., and Roddy, A. B. (2018). Genome downsizing, physiological novelty, and the global dominance of flowering plants. *PloS Biol.* 16 (1), e2003706. doi: 10.1371/journal.pbio.2003706

Simonin, K. A., Roddy, A. B., Link, P., Apodaca, R., Tu, K. P., Hu, J. I. A., et al. (2013). Isotopic composition of transpiration and rates of change in leaf water isotopologue storage in response to environmental variables. *Plant Cell Environ.* 36 (12), 2190–2206. doi: 10.1111/pce.12129

Song, Y., Poorter, L., Horsting, A., Delzon, S., and Sterck, F. (2021). Pit and tracheid anatomy explain hydraulic safety but not hydraulic efficiency of 28 conifer species. *J. Exp. Botany* 73(3), 1033–1048. doi: 10.1093/jxb/erab449

Sperry, J. S., and Tyree, M. T. (1988). Mechanism of water stress-induced xylem embolism 1. *Plant Physiol.* 88 (3), 581–587. doi: 10.1104/pp.88.3.581

Sprengel, C. K. (1996). "Discovery of the secret of nature in the structure and fertilization of flowers," in *Floral biology: studies on floral evolution in animal-pollinated plants*. Eds. D. G. Lloyd and S. C. H. Barrett (Boston, MA: Springer US), 3–43.

Teixido, A. L., and Valladares, F. (2014). Disproportionate carbon and water maintenance costs of large corollas in hot Mediterranean ecosystems. *Perspect. Plant Ecology Evol. Systematics* 16 (2), 83–92. doi: 10.1016/j.ppees.2014.02.002

Théroux-Rancourt, G., Roddy, A. B., Earles, J. M., Gilbert, M. E., Zwieniecki, M. A., Boyce, C. K., et al. (2021). Maximum CO2 diffusion inside leaves is limited by the scaling of cell size and genome size. *Proc. R. Soc. B: Biol. Sci.* 288 (1945), 20203145. doi: 10.1098/rspb.2020.3145

Tyree, M. T., and Hammel, H. T. (1972). The measurement of the turgor pressure and the water relations of plants by the pressure-bomb technique. *J. Exp. Bot.* 23 (1), 267–282. doi: 10.1093/jxb/23.1.267

Tyree, M. T., and Zimmermann, M. H. (2013). *Xylem structure and the ascent of sap* (New York: Springer Science & Business Media).

Warton, D. I., Wright, S. T., and Wang, Y. (2012). Distance-based multivariate analyses confound location and dispersion effects. *Methods Ecol. Evol.* 3 (1), 89–101. doi: 10.1111/j.2041-210X.2011.00127.x

Waser, N. M., and Price, M. V. (2016). Drought, pollen and nectar availability, and pollination success. *Ecology* 97 (6), 1400–1409. doi: 10.1890/15-1423.1

Wheeler, J. K., Sprerry, J. S., Hacke, U. G., and Hoang, N. (2005). Inter-vessel pitting and cavitation in woody rosaceae and other vesselled plants: a basis for a safety versus efficiency trade-off in xylem transport. *Plant Cell Environ.* 28 (6), 800–812. doi: 10.1111/j.1365-3040.2005.01330.x

Zhang, F. P., and Brodribb, T. J. (2017). Are flowers vulnerable to xylem cavitation during drought? *Proc. R. Soc. B-Biological Sci.* 284 (1854), , 20162642–20162650. doi: 10.1098/rspb.2016.2642

Zhang, F. P., Cairns Murphy, M. R., Cardoso, A. A., Jordan, G. J., and Brodribb, T. J. (2018). Similar geometric rules govern the distribution of veins and stomata in petals, sepals and leaves. *New Phytol.* 219 (4), 1224–1234. doi: 10.1111/nph.15210

Zhang, F. P., Zhang, J. L., Brodribb, T. J., and Hu, H. (2021). Cavitation resistance of peduncle, petiole and stem is correlated with bordered pit dimensions in magnolia grandiflora. *Plant Divers.* 43 (4), 324–330. doi: 10.1016/j.pld.2020.11.007